



HAL
open science

District MODeller and SIMulator (DIMOSIM) – A dynamic simulation platform based on a bottom-up approach for district and territory energetic assessment

Enora Garreau, Yassine Abdelouadoud, Eunice Herrera, Werner Keilholz, G.-E. Kyriakodis, Vincent Partenay, Peter Riederer

► To cite this version:

Enora Garreau, Yassine Abdelouadoud, Eunice Herrera, Werner Keilholz, G.-E. Kyriakodis, et al.. District MODeller and SIMulator (DIMOSIM) – A dynamic simulation platform based on a bottom-up approach for district and territory energetic assessment. *Energy and Buildings*, 2021, 251, pp.111354. 10.1016/j.enbuild.2021.111354 . hal-04116916

HAL Id: hal-04116916

<https://hal.science/hal-04116916>

Submitted on 22 Jul 2024

HAL is a multi-disciplinary open access archive for the deposit and dissemination of scientific research documents, whether they are published or not. The documents may come from teaching and research institutions in France or abroad, or from public or private research centers.

L'archive ouverte pluridisciplinaire **HAL**, est destinée au dépôt et à la diffusion de documents scientifiques de niveau recherche, publiés ou non, émanant des établissements d'enseignement et de recherche français ou étrangers, des laboratoires publics ou privés.



Distributed under a Creative Commons Attribution - NonCommercial 4.0 International License

1 **DIstrict MOdeller and SIMulator (DIMOSIM) - A dynamic simulation platform**
2 **based on a bottom-up approach for district and territory energetic assessment**

3 Enora Garreau¹, Yassine Abdelouadoud¹, Eunice Herrera¹, Werner Keilholz¹, G-E Kyriakodis^{1,2}, Vin-
4 cent Partenay¹, Peter Riederer^{1*}

5 ¹ Centre Scientifique et Technique du Bâtiment, 290 Route des Lucioles, 06 904 Sophia Antipolis,
6 France

7 ² LaSIE UMR CNRS 7356, Université de La Rochelle, Av. M. Crépeau, 17042 La Rochelle Cedex 1,
8 France

9 **Abstract**

10 The building sector consumes more than one third of the total final energy in the world. In order to tackle this is-
11 sue, new UBEMs (Urban Building Energy Modeller) are developed to simulate, analyse or optimise the energy
12 consumption at building and district scale. Such tools are useful for decision makers and urban planners, for the
13 design, retrofit or energy management of districts and their energy systems. This paper describes DIMOSIM
14 (District Modeller and SIMulator), a modular UBEM to design and optimize district energy concepts. Based on
15 an object structure, this tool creates a district from a GIS-file, completes missing data, simulates the buildings,
16 systems and occupancy under a given weather to finally assess the simulation outputs. Thanks to the modular
17 structure, it can be coupled to other tools to broaden the applications, as the simulation of microclimate or the
18 use of model predictive controllers to optimize the control of districts. Several case studies are proposed, illus-
19 trating various applications of DIMOSIM.

20 **Keywords**

21 Bottom-up, urban building energy modelling, energy assessment, neighbourhoods, building energy systems

* Corresponding author: DIMOSIM Team – address: Centre Scientifique et Technique du Bâtiment, 290 Route des Lucioles, 06 904 Sophia Antipolis, France – e-mail address: dimosim@cstb.fr

Abbreviations : CHP, Combined heat and power unit; COP, Coefficient of Performance ; DESTEST, District Energy Simulation Test ; DHW, Domestic Heating Water; DIMOSIM, DIstrict MOdeller and SIMulator; KPI, Key Performance Indicator; UBEM, Urban Building Energy Modelling; WWRS, Waste-water recovery system

22 1 Introduction

23 The building sector is one of the most energy consuming sectors in the world, consuming over one third of the
24 final energy [1]. Continuous urbanization and climate change will lead to an estimated 68% of the world's popu-
25 lation residing in cities in 2050 [2]. To mitigate the impact of these trends, new ambitious energy and urban de-
26 velopment objectives are set by authorities to improve buildings efficiency, reduce their consumption and im-
27 prove users' energy awareness. In order to translate these objectives into concrete action plans, the simulation
28 and analysis of district energy consumption and production are crucial. These approaches require both a detailed
29 level of building-scale modelling and a representation of the interactions that arise at the district-scale. Indeed,
30 various objectives coming from the political sphere, distribution system operators, energy producers or energy
31 planners require numerous simulations models and their optimisation. However, analysis and optimisation at the
32 district level in terms of energy, environmental, economic or social performances are very complex. This com-
33 plexity lies in the fact that it is a multi-scale problem with multi-energy systems, various usages and multiple
34 criteria to satisfy. The purposes of such simulations can range from buildings retrofit potential ([3]) to design
35 and sizing of thermal and/or electrical network ([4], [5]), to the assessment of renewable potential ([6]) or to the
36 solar and thermo-radiative calculation ([7], [8]). Other simulations focus on the thermal comfort [9], the design
37 and management of multi-energy systems or the development of optimised control algorithms (mainly predic-
38 tive) to increase energy flexibility ([10]–[12]) and/or energy savings [13]. Moreover, at a district and city level,
39 other phenomena can be taken into account, such as the microclimate ([14], [15]) or in case of district energy
40 networks fluid dynamic aspects ([4], [5]). These aspects can strongly influence energy consumption at several
41 levels.

42 The variety and complexity of modelling combined with the scale, the various aims of the simulation and the
43 limited availability of data suggests the need to develop a new integrated approach as classic dynamic thermal
44 simulation programs cannot adequately respond to these challenges. The growing interest in this type of simula-
45 tion leads to the development of new tools based on different approaches to assess the building demand or the
46 systems energy consumption. Allegrini et al. [16] proposed a review of several district-scale energy simulation
47 tools, separating them into 3 main fields of application: district energy systems, renewable energy generation or
48 urban microclimate assessment. For example, Fonseca et al. [17] developed CityEnergyAnalyst, an integrated
49 framework that focuses on optimizing building energy systems at district scale in with various models for sys-
50 tems, a resource availability procedure and multi-criteria assessment but lacking detailed models for heating and
51 electrical networks and multizone simulations. Berthou et al. [18] built another UBEM tool, SMART-E, that al-

52 lows to simulate a high number of buildings but with no aspect of thermal network or electric grid. Robinson et
53 al. [19] created CitySIM allowing to calculate the heating and cooling loads and energy consumption, including
54 a detailed solar mask calculation but with simpler systems and networks models. Chen et al. [20] developed
55 CityBES, an open web-based tool using EnergyPlus and city datasets to simulate urban area for building retrofit
56 analysis. As they respond to different objectives, every simulation platform has his own specific features.

57 Following the analysis of such simulation tools and their responses to the variety of objectives in a district simu-
58 lation, the bottom-up tool DIMOSIM (DIstrict MOdeller and SIMulator) was developed by the CSTB (Centre
59 Scientifique et Technique du Bâtiment) and is presented in this paper. The main objective is to be able to simu-
60 late any possible combination of systems, models and buildings at different scale (building, district or city), at a
61 high speed and in a modular and flexible way in order to respond to a broad spectrum of applications. DIMOSIM
62 allows the analysis of feasibility, conception and operation of district energy systems by considering and imple-
63 menting a wide range of phenomena for the transient analysis. It was partially validated with the ASHRAE
64 BESTEST and is part of the IBPSA Project One for creation of DESTEST validation [21].

65 DIMOSIM was previously presented by Riederer et al. [22]. It was originally developed in the context of the Eu-
66 ropean Resilient [23] and Smart Med park projects and is now used in various European and French collabora-
67 tive research projects. It was for example used in the E2District project [24] for the modelling of various district
68 heating systems and their management, but also in Sinfonia [25] for the retrofit analysis of districts. In the Resil-
69 ient project [23], DIMOSIM allowed to simulate and evaluate solutions combining renewables, storage and ICTs
70 for intelligent energy management at district level. In the framework of the Thermoss project [26], innovative
71 control optimization modules have been tested and related performances have been analysed. In the ADEME-
72 funded SHAPE project [27], DIMOSIM was deployed to train a simplified energy model that is then integrated
73 in a municipality-level refurbishing optimization algorithm. Some specific uses of DIMOSIM are presented in
74 papers ([28]–[31]).

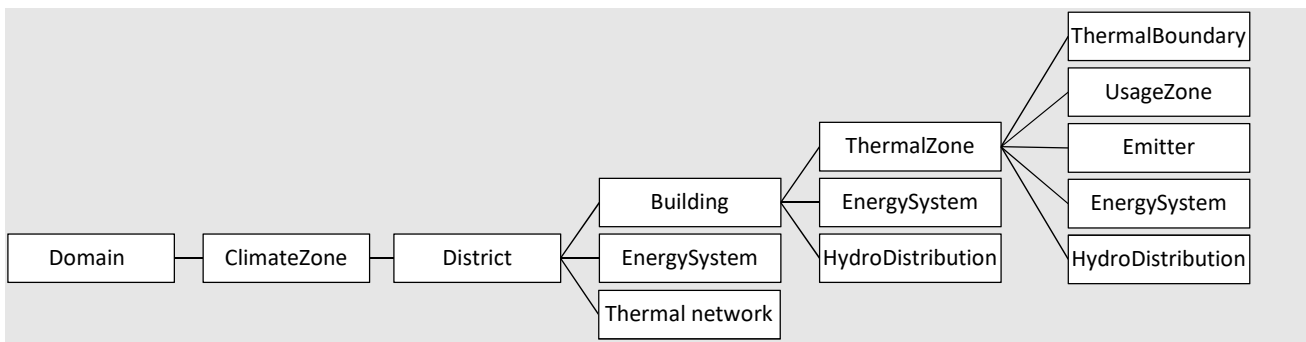
75 This paper is structured as follows: a first section introduces the general approach implemented in DIMOSIM, its
76 structure and the simulation procedure. The next sections are divided into the different steps that compose a typ-
77 ical study procedure: section 3 presents the object creator functions, section 4 the sizing function, section 5 the
78 simulation part, section 6 the assessment of the simulation outputs. Finally, section 7 shows some applications
79 on real case studies.

80 2 Methodology

81 2.1 DIMOSIM object-oriented structure

82 DIMOSIM is object-oriented, based on the concepts of objects and inheritance, where the objects contain data
83 and procedures that will pass to the connected sub-objects like a parent to children connection. This program-
84 ming paradigm allows to create an object-oriented structure from the parameters stored in input files and to easi-
85 ly produce the outputs for each component.

86 All classes in DIMOSIM are derived from a common generic object class, which contains methods to create the
87 object tree structure, to schedule the simulations and to access the results. Although the DIMOSIM objects are
88 all children of the generic object classes, they are also related to geographical area, systems, occupation or ther-
89 mal components. A “linked” relationship is created to connect several classes to each other, allowing a flexible
90 object structure. For example, a district heating network is linked to a district generator but is not a children or
91 parent of it.



92
93 Figure 1: Part of the object structure of DIMOSIM

94 As shown in the layout, the simulated domain can be composed of different climate zones (ClimateZone) allow-
95 ing to simulate projects broad enough to consider variation in weather or climate. Each ClimateZone can contain
96 different districts (District) including several buildings (Building). Different global or local energy solutions can
97 exist on any level, district, building or zone level. The Building is composed of thermal zones (ThermalZone)
98 where it is possible to find parameters and data about the thermal properties (ThermalBoundary and InnerMass)
99 and the occupancy (Occupant, Equipment and Vehicle in the UsageZone class).

100 The distinction between district-level, building-level or zone-level systems is done in order to connect automati-
101 cally the hydronic loops with the substations or the thermal zones according to the correct operation mode and
102 their balance.

103 In each procedure step, dependencies are defined to automatically launch the functions and methods in the nec-
104 essary order, depending on the step.

105 **2.2 *Model template***

106 The object structure presented before is the foundation of the simulation procedure and the modelling procedure
107 implemented in DIMOSIM. When defining a new generic class, several characteristics are set as the global pa-
108 rameters, the linked objects, the dependencies with other models or the states calculated in the functions of the
109 model. The resulting sub-objects, depending from the generic class, include the characteristics of their linked
110 parents. Additionally, *object creator*, *sizer*, *simulator* and *assessment* procedures are defined for each class.

111 By providing dependency management mechanisms as well as generic utilities (support for several input file
112 formats, result aggregation and plotting, object-tree data queries), DIMOSIM allows a fast prototyping of new
113 models and their integration in an inter-dependent simulation chain. Indeed, for each model an attribute defining
114 its dependencies on other models is created, automatically allowing the definition of the right execution order.

115 This modularity gives the ability to couple different generators at several levels, linking them automatically with
116 hydronic connexions to cover usages such as heating, cooling and domestic hot water. The related electricity
117 production (in case of CHP), energy storage and energy consumptions can be then calculated. It is possible to re-
118 trieve the outputs at all levels of the district for analysis and optimisation of each component.

119 **2.3 *Modelling and simulation procedure***

120 **2.3.1 *Input data***

121 A complete configuration is considered as ready to launch when all the needed input data (from the intrinsic pa-
122 rameters like the building geometry or the thermal properties, to the time-dependent profiles such as the weather
123 or the occupancy) are available in the appropriate data format. As in real life the gathering of all the data is very
124 complicated for an entire district, DIMOSIM has been developed in order to be compatible with a pre-processor
125 that is able to enrich the missing data necessary for the simulation. This pre-processor called QIRIEL [32] is
126 built upon French national data bases and completes the data for buildings (U values, solar coefficient, infiltra-
127 tion rate...), dwellings or occupants and their respective equipment according to their geographical situation and
128 construction year.

129 DIMOSIM can handle several input data formats such as CityGML or user-defined files. To generate building
130 geometries, DIMOSIM is only using the geometrical footprint and their associated heights (building height and
131 altitude) but is currently not considering roofs shapes.

132 The spatial scale of the district simulation ranges from small neighbourhoods to entire cities. Theoretically the
133 tool has been conceived to simulate very large districts, but with restrictions to the number of stored variables
134 for the analysis. However, this restriction depends only on the chosen hardware configuration. In order to have a
135 simulation adapted to a particular scale and objectives, DIMOSIM is flexible enough to change from rather simple
136 to detailed modelling. This can reduce computational time, but the modelling level must be chosen depending
137 on the required precision of simulation results.

138 Once the general parameters fixed (e.g. time step, simulation period, choice of model types, activation of modules...)
139 and the buildings defined (e.g. thermal parameters, occupancy, equipment and systems), the district will
140 be set as a children of a climate zone. If existing, district energy systems (thermal network, district generators,
141 electricity network) can be implemented with their location and their layout for the networks (details can be
142 found in the section on energy networks).

143 2.3.2 *Time and environment*

144 As district energy simulation can cover various simulation objectives over different time horizons , from several
145 days for control studies to several years for energy planning, the simulation tool proposes different levels of detail
146 in the model. The time step can be set by the user and has typical values in a range of minutes up to hours.
147 Even if the time step can be chosen in the order of seconds, DIMOSIM is not supposed to be applied for the
148 study of stability of electricity networks. Also, the use of very small time steps will lead the modeller to wrong
149 conclusions since the used transient models have not been developed for such small time steps.

150 The main principle of solving the global system problem is based on successive calculation of all objects while
151 the order of execution is automatically managed by the tool, based on the dependencies of the objects. For several
152 objects where the accuracy is critical, iteration functions are implemented in order to ensure correct calculation.
153 A global iteration loop has been recently added which allows the convergence at each time step using a
154 successive substitution method.

155 2.3.3 *Object creator procedure*

156 When all the known parameters are loaded, the *object creator* procedure is launched to create the DIMOSIM objects
157 from the input data. This procedure generates the buildings (in a grid shape district if none are indicated in
158 the input file), the geometry of the thermal boundaries, the thermal zones and their systems, and calculates the
159 adjacency between zones and buildings. It creates and optimizes also network layout (connections and distances).
160

161 2.3.4 *Sizing procedure*

162 The aim of the sizing procedure is, starting from all objects created, to set parameters related to the physical size
163 of the object (e.g. nominal power of a boiler etc.). It imports all available parameters and allows to define appro-
164 priate parameters of all models of objects. It generates the electrical and thermal loads coming from the occupant
165 activities in buildings, and calculates the thermal heating, cooling and DHW nominal demand for each zone and
166 building based on the relevant set-points (e.g. temperatures). From these nominal demands, the parameters of all
167 components are sized starting from the emitters, hydronic networks up to the generators (at zone, building and
168 district level).

169 2.3.5 *Simulation procedure*

170 This procedure is based on the concept of dependencies where the objects are used to hold information in a
171 structured way (district parameters, simulation parameters and current results). Before launching a simulation, it
172 is necessary to check whether an object has a simulator attribute and whether all its dependencies have finished
173 their simulation (the simulation of occupants for example has no dependency from other models and is thus run
174 without the need of waiting any other simulators). If this is the case the simulation for this object can be
175 launched, otherwise it passes and collects again the method in the call back list till all the dependencies are fin-
176 ished. Once the last dependency finished, the simulation of the current object is authorised to run. This concept
177 is actually applied in each procedure (object creator, sizer, simulator and assessment), but is the most complex
178 for the simulator part, where many function and dependencies are used.

179 Before simulating any thermal model, the radiations are computed with the solar mask providing solar gains for
180 each thermal zone (separated in diffuse and direct parts) on the envelope and on the windows.

181 During the simulation, the models are called at each time step, in sequence or in a global matrix equation system
182 (if the components require it) based on the results of the previous time step. To avoid parameter setting of con-
183 trollers, iteration methods on ideal control signals has been implemented. The relevant outputs are saved for the
184 current time step in a data output structure. They can be accessed at the end of the simulation for the evaluation
185 of system performances in terms of energy efficiency, emissions and costs.

186 2.3.6 *Assessment procedure*

187 Once the simulation is finished and all data available, different types of outputs are generated: either the raw
188 outputs representing key states and fluxes or post-processed outputs. With databases related to external factors
189 (as price per energy unit) it is possible to compute new relevant key performance indicators (KPI). This proce-

190 dure enables the automatic post-processing of outputs at different levels such as zone, building or district while
191 applying the right assessment procedure (such as averages for temperatures, sums for fluxes etc.).

192 **2.4 Implementation**

193 DIMOSIM is implemented as an object-oriented Python 3 package with continuous integration and deployment
194 capabilities, simplifying the implementation of new models and the delivery of applications while always guar-
195 anteeing the correct operation with unitary and functionality tests.

196 DIMOSIM is a python package (i.e. a collection of sub packages and modules accompanied by an installer). As
197 such, it can be used in different ways:

- 198 - Interactively in a python Notebook
- 199 - Imported in a user-defined script and launched by the python interpreter; this can be useful for studies,
200 including parametric runs.
- 201 - Imported in another package; this is a typical use case for implementing extensions or more complex
202 applications based on DIMOSIM.
- 203 - Via a REST API over a http connection, using the included web application; this mode of operation is
204 used by online applications and / or services targeting end-users, such as Powerdis or Urbanprint [33]

205 Efforts have been made to automatically translate DIMOSIM by using the Cython compiler [34], yielding a sig-
206 nificant increase in execution speed (around 30 up to 60 times faster) and an advantage in energy consumption
207 [35]. Using a computer with an i5 core 2.5 GHz and 8 Gb RAM, the simulation (object creator, sizer, simulator
208 and assessment) of one building for one year and a 1 H time-step takes 4 seconds. For a dense district (with
209 many adjacent buildings) with 100 monozone buildings and local distribution (no thermal network), the simula-
210 tion takes 84 seconds.

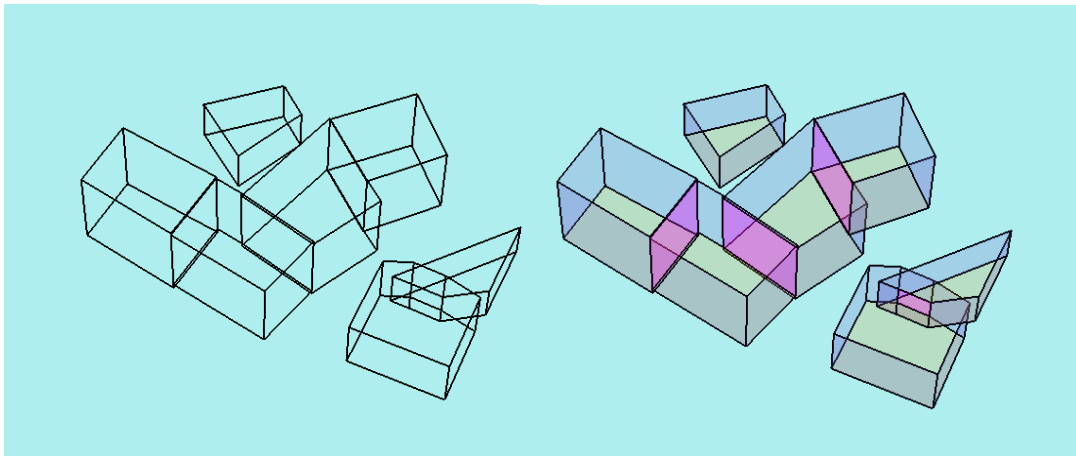
211 DIMOSIM is not an open-source tool and cannot be accessible through commercial license. However, Efficacy
212 plans to offer a web application running with DIMOSIM as the computing core (but with less available features).
213 For research projects, direct use of DIMOSIM can be done through research agreements and/or common pro-
214 jects.

215 **3 Object creator**

216 **3.1 Boundaries and adjacency**

217 The boundaries are created either from arrays of boundary surfaces and azimuths (exterior and inner boundaries)
218 or from the footprints and heights of each zone or building. For the latter, a simple geometrical procedure allows
219 to obtain surface, azimuth, inclination and centre of each boundary.

220 At the same time the geometry is created, a module detects adjacent envelope elements (horizontal and vertical)
221 which also allows to define if the current element is exposed to solar radiation. For example, in Figure 2 the pink
222 adjacent walls are detected and defined as InnerWall objects. Thermal adjacency between buildings is dealt for
223 now as adiabatic: the thermal mass of the inner boundaries is lumped to the internal mass of the building in order
224 to correctly represent thermal inertia, but no heat transfer is modelled. For the next version, thermal exchanges
225 between zones are currently being implemented.



226
227 Figure 2: Adjacencies calculation

228 These boundaries can be taken into account as separate boundaries/objects but the exterior walls can also be
229 grouped (aggregated) into one unique object to be represented as only one boundary in the thermal model to
230 speed up the simulation.

231 **3.2 Zone and Building configurations**

232 Depending on the input data, either thermal zones are created if the buildings have been defined, or vice-versa.
233 Several DIMOSIM system configurations are implemented, in order to create automatically all the system loop,
234 from the emitter to the generator with the possible linked hydraulic distribution. It prevents any duplicate sys-
235 tems. The system object creator takes a json file from a system library linked to the specified configuration, cre-

236 ates the corresponding objects by adding them to the relevant level (zone, building or district) and connects them
237 with the hydronic loop.

238 If a usage zone is provided, the object creator adds a usage type to the thermal zone (housing, office, shop, pri-
239 mary school...), that will be later sized and then be used for the nominal DHW draw-off power. It is also possi-
240 ble for the user to use a function that creates equipment and occupants of a dwelling using either its surface or its
241 number of rooms, based on a French database.

242 **4 Sizer**

243 **4.1 Climate zone**

244 DIMOSIM can read several weather data file types such as epw or tmy. Weather data in these files can be based
245 on typical meteorological data, on-site measurements, or from any other weather data generator. They must con-
246 tain the time-series of ambient temperature, relative air humidity, diffuse and direct solar radiation as well as ef-
247 fective sky temperature. If the sky temperature is not available, it can be either replaced by the exterior tempera-
248 ture or calculated as in the EnergyPlus simulator [36]. The ground temperature can be taken as constant or can be
249 modelled by the Kasuda [37] equation as a sinusoid.

250 **4.2 Thermal zone**

251 The thermal boundary sizer uses default values for boundaries missing parameters, and converts, if not specified
252 directly, the U-value, inertia and insulation parameters to layers with their associated thickness, density, specific
253 heat and conductivity. The position of the insulation can be chosen between indoor, outdoor or infill in order to
254 correctly represent thermal inertia for all exterior boundaries. Additional parameters as heating and cooling tem-
255 peratures set-points and air change due to ventilation and/or infiltration are also set in this sizer. Once all data
256 defined, the nominal heating and cooling demands of the thermal zones are calculated based on the exterior tem-
257 perature data (T_{ext}). These thermal demands ($D_{tz\ heating}$, $D_{tz\ cooling}$ – Eq. 2, Eq. 3) are calculated from the building
258 equivalent U-value ($U_{building}$ based on surfaces S , Eq. 1), the infiltration rate (\dot{m}_{infil}) and the set point tempera-
259 tures ($T_{heating}$ and $T_{cooling}$). For the cooling demand, the solar gains through the window surface (Q_{solar}) and in-
260 ternal gains (G_{int}) are taken into account because of its higher sensibility.

$$U_{building} = \sum U_{bound} * S_{bound} \quad Eq. 1$$

$$D_{tz\ heating} = \left(U_{building} + \frac{\dot{m}_{infil}}{3600} c_{p\ air} \right) * (T_{heating} - \min(T_{ext})) \quad Eq. 2$$

$$D_{tz \text{ cooling}} = \left(U_{building} + \frac{\dot{m}_{infil}}{3600} c_{p_{air}} \right) * (\max(T_{ext}) - T_{cooling}) + S_{window} * \frac{\max(Q_{solar})}{3} + G_{int} \quad Eq. 3$$

261 4.3 Generation and distribution

262 **Emitters:** The nominal parameters of emitters are calculated from the zone demand for each operating mode
 263 (DHW, heating, cooling or reversible), depending on the type of emitter. In the case of hydronic emitters, nomi-
 264 nal thermal output, nominal temperature difference between supply and return (ΔT_{nom}), nominal flow rate
 265 ($\dot{m}_{nom \text{ emitter}}$) and the overall heat transfer coefficient are defined.

$$P_{nom \text{ heating}} = D_{tz \text{ heating}} * \alpha_{oversizing} \quad Eq. 4$$

$$\dot{m}_{nom \text{ emitter}} = \frac{P_{nom \text{ heating}}}{c_{p_{water}} \Delta T_{nom}} \quad Eq. 5$$

266 **DHW system:** The DHW sizer calculates the nominal parameters such as the flow rate or the supply temperature
 267 from either the zone parameters and the occupants present in the dwellings, or from a custom profile.

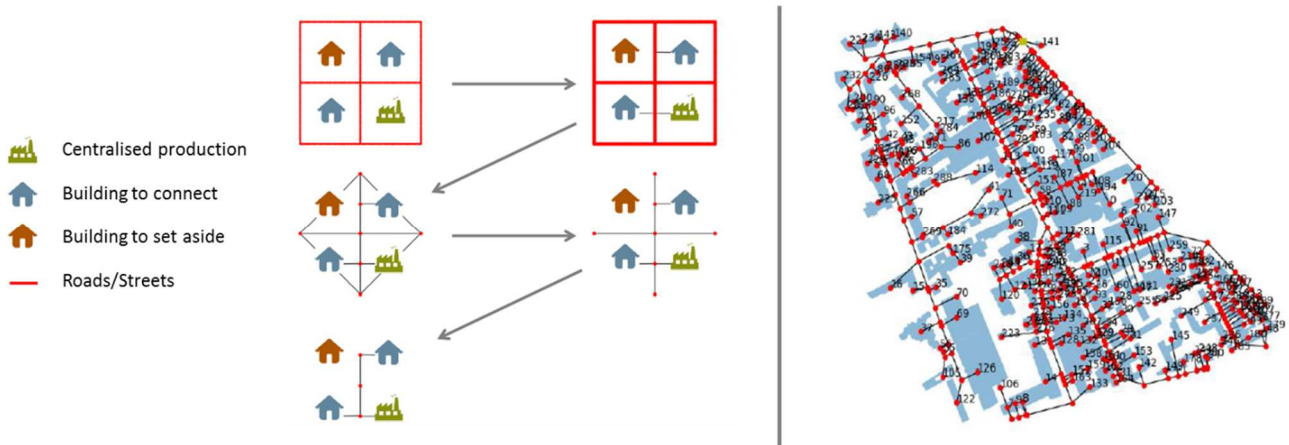
268 **Hydronic distribution:** Two types of distribution are implemented and automatically linked with the generators
 269 at different scales: a local hydronic distribution at the zone level connecting the emitter and the zone generator
 270 (or zone substation) and a central distribution at building-level connecting the building generator or substation to
 271 the zones. These distributions collect the parameters of the sub-objects to calculate the nominal parameters and
 272 the global generators operating mode.

273 **Heat, cold, hot water and electricity generation:** When simulating a district, the thermal production of genera-
 274 tors can be implemented at different scales: at the thermal zone level, as an individual local system, at the build-
 275 ing level as a collective local system or at the district level as a centralised production. The generation models in
 276 DIMOSIM are the same for central or decentralised systems but their connections differ from one to another.
 277 The main parameters are set by the user (nominal performances as efficiency or COP, fuel type...) and the nomi-
 278 nal powers, temperatures and flow rate are derived from the hydronic distribution that links the generator to the
 279 next, lower level. In addition, a thermal storage can be implemented as a water tank to store any thermal loads
 280 from the generators.

281 **Ventilation:** The sizer for the ventilation object is rather simple. It completes the missing parameters by default
 282 values, if not specified by the user in the input file, such as the air change rate (during day and night) and the ef-
 283 ficiency, depending on the type of ventilation of the thermal zone (mechanical ventilation with or without heat
 284 recovery etc.).

285 **4.4 Thermal network**

286 A district thermal network is simulated either for a conception-study or an operation-study. To respond to these
287 two objectives, the network can be modelled in two different manners: from user-defined data (existing network)
288 with path coordinates and thermal insulation, or using an automatic method that generates the network paths
289 based on the roads in the district. For this second method, an optimised network structure is calculated using a
290 minimum spanning tree method. This method searches the optimal network (cost criteria) of the road network to
291 connect all buildings and productions, while removing all unnecessary and/or redundant connections (Figure 3).
292 A thermal network can also have several sub-networks that can be linked via district substations, for example to
293 manage different supply temperatures for specific areas or to add additional generators in sub-networks.



294

295 Figure 3: Automatic generation of thermal network - principle and application on the French BDTOP0 [38]

296 After the creation of the network flow path, the second part of the sizing creates the length, nominal flow and
297 thermal mass matrices for the network model. Again, two types of distribution network models are available in
298 DIMOSIM in order to match with the simulation objectives:

- 299 - A detailed model that considers all tube segments with their individual characteristics. To do so, the siz-
300 ing procedure uses the previously created graph and generates first the length matrix L. In this matrix,
301 distances between the nodes are stored in an order that suits the calculation models. Then, a flow matrix
302 of the same size as L is created, with the same order by retrieving the nominal flow rates from the sub-
303 stations. The tubes are initialized with the calculation of the sections, U-values and thermal mass, each
304 of them stored in a separate matrix of the same size as L. A final UA matrix specifies the overall loss
305 coefficient per unit area for the pipe segments. Internal heat transfer between fluid and internal surface
306 of the pipe is assumed as perfect.

307 - A simple model consisting of an equivalent single-output tube (aggregated) created as an equivalent of
308 all the given tubes under the nominal conditions (the simple model is calibrated to match the thermal
309 losses calculated using the detailed model at nominal conditions). This model suits for feasibility studies
310 where transients are not required, and fast simulation speed is needed.

311 **5 Simulator**

312 **5.1 Occupation**

313 The electricity consumption in a district is related to the occupancy, notably from the use of electric equipment
314 and lights. Two approaches are proposed in DIMOSIM for the occupancy:

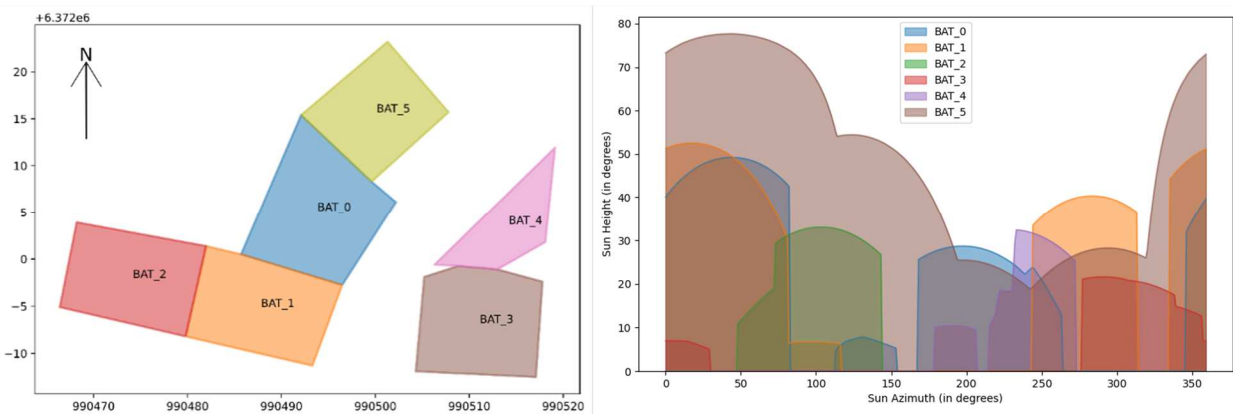
315 - Using custom usage zones with sizing coefficients, which propose custom profiles of internal gains,
316 electric loads, DHW draw-off, and temperatures and air change rate set-points, following the zone usage
317 and usable floor area, and based on the day of the year (week, week-end or holidays).

318 - Using a pre-processor for residential buildings, called Croniq [39] , based on measurement data (data-
319 base from the survey “Enquête emploi du temps” from french INSEE [40]) with stochastic approach.
320 From these measurement data, stochastic occupancy profiles are created with 10-min time step. The
321 number of occupants can be imposed by the user, otherwise it is determined from the dwelling usable
322 area. For each occupant and following its status (student, worker...), a schedule of activity linked to
323 equipment and lights is created from the stochastic profiles (each activity is linked to an equipment), in-
324 volving load profiles for the electrical equipment and for the zone. The tool, directly implemented as a
325 module in DIMOSIM, only allows to generate occupancy profiles for the residential sector. For other
326 building sectors, the availability of data is very low and the multitude of zone usages is very complex.
327 Once this data gathered, it could be implemented in Croniq. For residential usage zones, the equipment
328 used by the occupant is divided into cooking (oven, cooktop, fridge...), housework (washing machine,
329 dryer...) and electronic devices (television, laptop...). Electric cars are also implemented as their use is
330 spreading. The module consistency was validated by Dréau et al. [41] with typical French values for
331 mean annual consumption [42] and the daily mean demand with Vorger results [43].

332 The lighting is implemented following the occupation and the solar radiation received by the building. The
333 blinds can be controlled following the operative temperature in the thermal zone during the day based on the
334 zone air temperature. Additionally, a ratio is used to consider the transparency of the shading devices. To date,
335 only external shading devices are implemented.

336 **5.2 Solar radiation**

337 A solar mask calculation module has been implemented as a pre-processor. This module calculates, for each
338 building, a 360° view of masks height around each point with an angle resolution of typically 1° (default value).
339 To improve the ray tracing, another discretisation is done on the vertices of all surrounding buildings in a de-
340 fined radius (typically 500 m) for the calculation. The further the neighbour building is, the less discretized are
341 the vertices. The ray tracing is calculated either at the centre of each zone (at mid-height), or at the centre of
342 each zone boundary (walls and roof). As an example, the masks at the centre of each building are presented for a
343 set of buildings in Figure 4. Then, for each time step of the simulation, the azimuth and altitude of the sun are
344 calculated, and the correct shading coefficient is applied to the direct radiation. The shading coefficients are also
345 used to compute a sky view factor for the long wave radiation. No reflexion between buildings is considered in
346 the current version.



347
348 Figure 4: Mask calculation between buildings (calculation at building center). For each building the shading
349 masks heights in degree are plotted (0° when there is no solar mask, 90° for full solar mask) with a 360° view
350 around the building.

351 The solar radiation calculation was compared with TRNSYS on one building, and with DAYSIM [44] in [29] on
352 several districts of different morphologies.

353 **5.3 Thermal district model**

354 **5.3.1 Structure**

355 The role of this module is to allow the simulation of all thermal phenomena of the district. To do so, the model
356 assembles the simulation models of all created objects. By assembling them, it creates specific data structures
357 holding all parameters of these objects and results arrays. At the same time, function factories are built in order

358 to assemble the unit models of each class in loops: first among the classes inheriting from a common generic
359 class and then considering all generic classes according to the dependencies.

360 This module makes extensive use of introspection techniques on the content of the objects descending from the
361 generic classes so that new classes and their associated models can be added without any modification to the
362 model.

363 After an initialisation phase that allows to set model parameters (e.g. matrix coefficients for the zone model
364 etc.), the thermal district model loops through all assembled unit models until convergence is reached for each
365 time step. Convergence is considered reached when the results from one iteration do not differ more than ε per-
366 cent from the previous iteration for all unit models. Controllers are computed only once for each time step and
367 are thus excluded from the iteration process. In the iteration procedure, outputs from the previous iteration must
368 be kept in memory for each object, before updating it when convergence is reached. For models maintaining
369 states (such as wall temperatures in a thermal zone for example), states are set once convergence reached at each
370 time step (at the last iteration).

371 5.3.2 Zone model

372 The thermal model is implemented as a state space approach and solved using the Exponential-Euler method:

$$\dot{X}(t) = A \cdot X(t) + B \cdot U(t) \quad \text{Eq. 6}$$

$$X^{n+1} = X^n \cdot e^{A \cdot dt} + \frac{e^{A \cdot dt} - I}{A} \cdot B \cdot U^n \quad \text{Eq. 7}$$

373 Where X is the state vector (function of time), A the constant state matrix, B the constant input matrix and U the
374 input vector and dt the time step. The thermal zone simulator creates, at each time step, the input vector U for
375 the state space model by assembling all internal, solar and emitter gains as well as the external boundary condi-
376 tions. It runs then the thermal zone state space using the A and B matrices obtained at the initialisation and the
377 state vector from the previous time step. The zone states are then used to define automatically the heating or
378 cooling mode for the next time step.

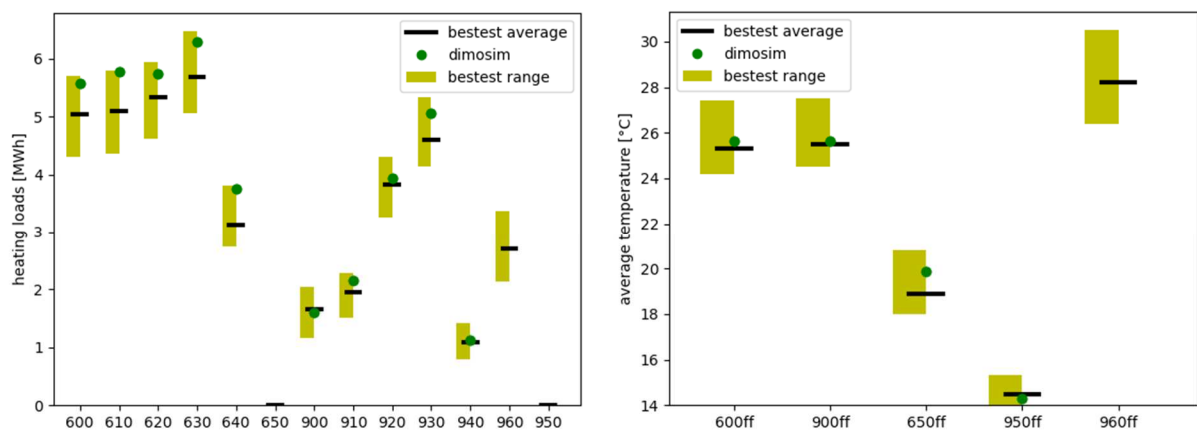
379 Based on the experience of several projects (with validation by Perez and al. [45]), a new building thermal model
380 was implemented, called a R_iC_j model. The R_iC_j model is represented in Figure 15 in the appendix. This model
381 adapts itself to the quality of input data and the objective of the modeler: it can either be simplified by grouping
382 the walls into one to reduce the computational time or detailed by simulating each envelope element individual-
383 ly. The generic envelope model (walls, floors or roofs) is composed of a minimum of 4 capacitors representing

384 external surface node, first mass layer node, second mass layer node and internal surface node connected via 3
 385 thermal resistances. The position of the insulation (model parameter) allows to correctly model transient thermal
 386 behavior of the envelope element. The user can choose a more detailed discretization scheme if more detail on
 387 the layers is available. This model is identical for the floor envelope, with the only difference that the floor is not
 388 exposed to solar radiation and that the floor is not linked to ambient conditions but the ground temperature. The
 389 thermal window model (convection, conduction and long wave radiation) aggregates all windows of a thermal
 390 zone. The nodes are connected to both air and mean radiant temperature of the thermal zone. Radiative absorp-
 391 tion and transmission at the windows are calculated for each orientation and considered as the sum over all ori-
 392 entations.

393 The ventilation module calculates heat flux from or to the zone by the ventilation system and from infiltration.
 394 Thermal bridges are estimated from the number of floors, the position of the insulation and the perimeter of the
 395 zone footprint considering a global thermal bridge coefficient. Finally, an internal mass is considered that repre-
 396 sents the thermal inertia of all adjacent and internal walls or floors. As already mentioned, in the current version
 397 of DIMOSIM heat exchange between zones is neglected and only thermal inertia of adjacent walls is considered.
 398 This is currently being updated in order to dispose of a real multizone building. This is typically important if the
 399 zones have different usages such as residential, commercial, office etc. with different set points. A more de-
 400 tailed description can be found in [15].

401 The zone states are represented via the air and mean radiant temperature nodes where convective and radiative
 402 heat gains are injected. The control of set points is based on a zone temperature sensor considering the average
 403 of both previous temperatures.

404 The model was validated with the BESTEST cases (ASHRAE): the Figure 5 shows DIMOSIM heating loads and
 405 average temperatures compared to the BESTEST averages and ranges.



406

407 Figure 5 : DIMOSIM building model against BESTEST cases (left : heating loads comparison, right : average temperatures
408 with free float simulations comparison)

409 5.3.3 Generation and distribution

410 **Emitter**

411 A generic, steady state emitter model is used to represent multiple systems as radiators, fan coil, heating floor,
412 etc. At each time step, using a nominal heat transfer coefficient UA_{nom} , the maximum thermal output is calculat-
413 ed based on the current state temperatures (T_{in} the hydronic distribution supply temperature and $T_{zone, op}$ the oper-
414 ative zone temperature):

$$\dot{Q} = UA_{nom} * (T_{in} - T_{zone,op}) \quad Eq. 8$$

415 From the estimated zone temperatures calculated in the R_iC_j model, the thermal output is taken as the ideal con-
416 trol value of heat flux in order to reach the set-point temperature. If the set-point cannot be reached (maximum
417 power too small or too high gains at emitter switched-off), the model calculates the zone states that can be phys-
418 ically reached.

419 **Distribution**

420 In case of a hydronic energy system, a hydronic distribution is used to distribute the supply water from either a
421 zone or building generator or substation to the zone emitters. The model is composed of a supply and return loop
422 and takes the thermal losses into account with a steady state approach. The loss coefficient is calculated from the
423 flow rate (\dot{m}) and the tube heat loss coefficient (UA) in Eq. 9, and is used to determine the tube outlet tempera-
424 ture (T_{out}) from the inlet temperature (T_{in}) and the surrounding exterior temperature (T_{ext}) in Eq. 10.

$$\alpha_{loss} = 1 - e^{-UA/(\dot{m}c_{pfluid})} \quad Eq. 9$$

$$T_{out} = (1 - \alpha_{loss}) * T_{in} + \alpha_{loss} * T_{ext} \quad Eq. 10$$

425 **Ventilation and infiltration**

426 Infiltration and two types of ventilation are implemented: simple mechanical extract ventilation and mechanical
427 ventilation with heat recovery. Based on a fixed heat recovery efficiency ε (0 for infiltration) the ventilation
428 simulator calculates the losses as a function of the mass flow rate of ventilation (\dot{m}), the exterior temperature
429 (T_{ext}) and air temperature of the zone (T_{air}):

$$Q_{ventilation,losses} = \dot{m} * cp_{air} * (1 - \varepsilon) * (T_{ext} - T_{air}) \quad Eq. 11$$

430 In case of mechanical ventilation, auxiliary energy consumption is estimated.

431 **Generators and thermal substations**

432 For the generators one or two sub-functions are used:

- 433 - A “supply” function, if the generator is hydronic, setting the inlet temperatures depending on the operat-
434 ing mode and available temperature of the generator. For all generators a heating or cooling law can be
435 chosen for the supply set-point temperature, linked to a heating law calculation function. Otherwise, a
436 constant set point is applied.
- 437 - A “calculation” function that is specific for each generator sub-class and that calculates states, return
438 temperatures and flow rates as well as consumption (specified by fuel type). For each level, different
439 generators are available (Table 1). These generators are based on physical models with data enrichment
440 based on experimental data and expert rules.

441 Table 1: Systems technologies in DIMOSIM

Zone	Building	District
Boiler	Boiler	Boiler
Air-water heat pump	Air-water heat pump	Water-water heat pump
Water-water heat pump	Water-water heat pump	Waste-water recovery system (WWRS)
Combined heat and power unit (CHP)	Combined heat and power unit (CHP)	Aquifer/ambient cooling Tower
Air-air heat pump		
Electric heater		

442 Like the other hydronic objects, the thermal water storage model is composed of a supply function that sets the
443 supply temperatures before calling the calculation loop. This latter module uses a well-mixed transient model
444 considering losses to a uniform environment with a constant heat loss coefficient and controlled with an on-off
445 controller.

446 *5.3.4 Thermal district network*

447 In a thermal network, two linked phenomena arise: the thermal and the hydronic behaviour. Indeed, the fluid
448 temperature has, in theory, an impact on pressure drops and flow rates. This impact can be necessary to model in
449 some cases, but is not necessary in many others. Therefore, the network model is available in two levels of de-
450 tail:

- 451 - A simple thermal network model only based on idealised flow and energy balances: this first version
452 collects idealised flow rates from the thermal substations and calculates back, by flow balances, the ide-
453 alised flow rates in all network segments. The main flow rate from the energy centre can be variable or
454 fixed. In the case of variable flow rate, the ΔT at the substation is fixed to its set-point and flow rate at

455 the substations are calculated from the energy balance. In case of a fixed flow rate, substation return
456 temperatures are calculated from the energy balance. Once all flow rates in the network calculated, the
457 global pressure drop at the energy centre is calculated from the pressure/flow rate relationship in the
458 whole network, allowing to estimate circulation pump electricity consumptions for the whole network.
459 An ideal hydronic balancing method is implemented to allow the calculation of the global pressure drop.
460 - A detailed, model, currently being implemented (which was already available in the first version pre-
461 sented in [22]), that calculates pressures and flow rates in all network segments. This version allows es-
462 pecially the calculation of meshed networks or networks with multiple generators at different locations.
463 In order to accelerate the simulation and avoid convergence problems with the pressure calculation, the
464 simulation resolution is based on parameters calculated in the previous time step (pipe friction factors
465 etc.).

466 For both methods, the pump operating point is determined by a match between the pump characteristic curve and
467 network pressure and flow rate. Pump consumption is then calculated from this result using a constant pump ef-
468 ficiency.

469 At the building or district level for thermal network, different types of heat exchangers for the substations are
470 available:

- 471 - An ideal exchanger that forwards the temperature at the substation primary circuit inlet to the substation
472 secondary circuit outlet (with the temperature being limited to the given supply set point temperature
473 following for example a specific heating curve of this sub-network).
- 474 - A more detailed heat exchanger with either parallel, counter-flow and crossflow exchanger models,
475 based on the NUT method. The UA factor is calculated during the initialisation in order to satisfy the
476 thermal exchange with the nominal parameters.
- 477 - A substation with a thermo-refrigerating heat pump to consider the heating and cooling mode at the
478 same time and delivering both, heating and cooling, to two separate secondary subnetworks. This heat
479 pump model is based on a characteristic efficiency polynomial function.

480 On the thermal side, again, three different tube models are implemented for the simulation of each network seg-
481 ment:

- 482 - A steady state and dynamic models as already presented in [22].

483 - A plug-flow model was added to better consider time delays and fluid inertia using Lagrangian ap-
484 proach: each elementary pipe is composed of variable-size fluid volumes. These volumes are pushed, in
485 the next time step through the network, following the flow rates and time step. The model computes the
486 loss of flow temperature to the ambient environment, no mixing or conduction is considered between the
487 segments. For a volume i , the following differential equation must be solved:

$$Cp_{fluid}M_i \frac{dT_i}{dt} = -UA_i(T_i - T_{env}) \quad Eq. 12$$

488 With M the mass of the fluid segment, UA the heat transfer coefficient of the segment and T_{env} the ground ambi-
489 ent temperature. The global model is then an assembly of tube models calculating the temperature distribution
490 throughout the thermal network and passing them to the building via the substations.

491 The thermal district network results were compared to real data in several projects, such as Thermoss project
492 [46], giving accurate results.

493 **5.4 Photovoltaics**

494 For a given field of photovoltaic panels on a roof, solar radiation is computed considering solar masks at the cen-
495 tre of the roof. Then, using the pvlib package, the effective irradiance on a defined module and the alternative
496 and direct current outputs are calculated. The power production finally is dependent on the cell temperature, the
497 area and position of the panels, the technical characteristics of the module, the effective irradiance and the ther-
498 mal losses. For now, only a unique module and inverter are implemented (but could be extended). Panel area, tilt
499 and the orientation must be defined by the user.

500 **5.5 Electric network and storage**

501 The electrical storage model calculates the electricity consumed and produced by the storage to minimize the op-
502 eration cost considering variable electricity prices [47]. The electricity prices can be implemented by the user or
503 default prices available for France, Germany and Switzerland can be used.

504 The active and reactive loads in the electrical network are gathered from all the buildings in the feeders, and the
505 transformer voltage is then retrieved for each of them. A CPP data model is created, the inputs are scaled accord-
506 ingly and a power flow calculation is launched on the CPP model to compute the global voltage, active and reac-
507 tive powers.

508 **6 Assessment**

509 For each object and on each level (zone, building and district) the outputs are calculated based on the sub-objects
510 they have, by aggregating the results from the lowest level to the highest. For each type of result, a dictionary is
511 implemented to choose the type of aggregation, the unit and the weight (ex: per surface) to use.

512 Two types of outputs are available: raw outputs and key performance indicators (KPI). The raw outputs are the
513 states of each object (e.g. temperature, control inputs and voltages), and the energy fluxes at each level (con-
514 sumption per fuel, energy production, renewable energy production, losses...). These raw outputs are used to
515 generate the KPIs which are divided into four modules: thermal indoor comfort, energy, power (per source and
516 usage) and the financial cost (investment, maintenance and annual cost).

517 As the states of every object are known, other KPI's can be implemented and the different profiles can be visual-
518 ized at each level of the district (emitter, thermal zone, building, generator, thermal network, district) or with a
519 specific selection of objects.

520 **7 Case studies**

521 This last section illustrates the main three use cases of DIMOSIM with existing projects as example. For each
522 use case, the objectives and the approach are described, followed by the presentation of the main outcomes.

523 **7.1 Building Energy Modelling**

524 *7.1.1 Presentation of the case study*

525 In this use case example, DIMOSIM has been used for a real case study in a city in the south of France. The city
526 was interested in a comparison of the impact of several technological solutions of the energy systems installed in
527 buildings on the district energy demand and the flexibility of the global energy system.

528 The district is composed of existing buildings (residential, service, commercial and a warehouse), and new build-
529 ings that are about to be constructed (residential and “mix” buildings composed of both residential and office ar-
530 eas). The total number of buildings is 227.

531 In order to simulate the buildings, the buildings geometry, the thermal properties of envelope and the type of oc-
532 cupancy in each of the buildings were gathered. The occupancy profiles were created as presented earlier, thanks
533 to the CRONIQ module. The French database BDTOPO® was used for the footprint of the existing buildings.

534 The thermal properties of the latter were taken either from French databases (PHEBUS, INSEE), or from energy

535 diagnosis of specific buildings. For the new buildings, the properties were chosen in accordance with the French
536 thermal regulation and its energy labels, and the building design from a french data base of submitted building
537 permits.

538 Five energy supply scenarii for the new buildings were created, in which the systems are differentiated per us-
539 age: for example, a mechanical ventilation (without heat recovery) for the dwellings, or air handling units for of-
540 fices. On the other hand, the office zones are always equipped with individual heating systems (only the fuel is
541 changing following the type of scenario). The five scenarii for the new buildings are mainly based on the choice
542 of the heating system and are:

- 543 - “Full electricity”: all dwellings and offices have their own individual electric HVAC systems (electric
544 convectors, reversible heat pump and thermodynamic water heater). A local PV production is placed on
545 half of the buildings.
- 546 - “Full individual gas”: all dwellings and offices have their own individual gas system (boiler, heat pump,
547 instantaneous DHW). A complementary electrical heat pump for cooling is installed for the offices. A
548 local PV production is placed on half the buildings.
- 549 - “Full collective gas”: the buildings are equipped with a central energy generator (boiler, heat pump,
550 DHW solar collector). As in the previous scenario an electrical heat pump for cooling for the offices is
551 used.
- 552 - “Smart gas cogeneration”: the buildings are supplied with CHP combined to a storage tank., As previ-
553 ously, an individual heat pump is used for cooling.
- 554 - “Smart gas hybrid”: Instead of a CHP system, a hybrid boiler (electric heat pump coupled with a gas
555 condensing boiler) is used for a collective supply in each building.

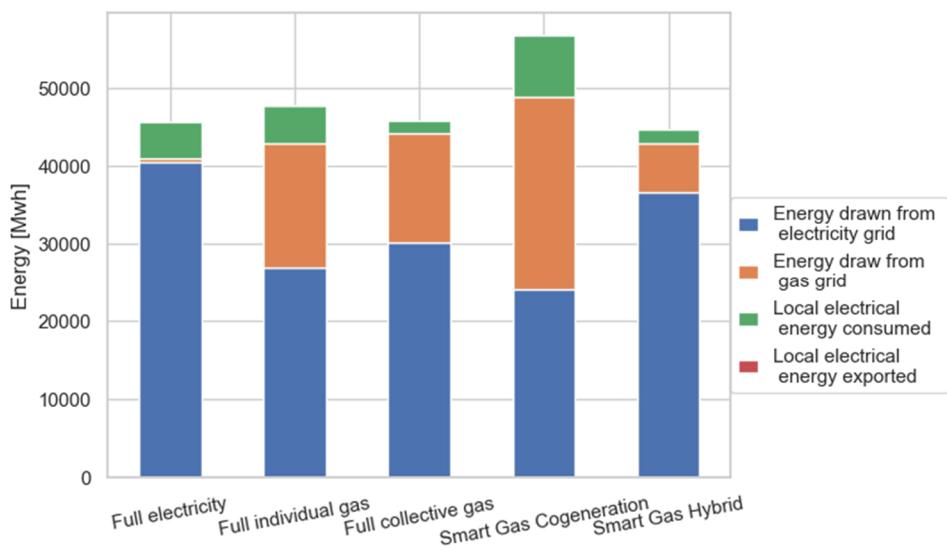
556 7.1.2 Results

557 DIMOSIM simulated the multi-zone buildings with the solar masks and occupancy for all scenarii with a 10-
558 minute time step. The assessment has been carried out based on the following simulation outputs: energy de-
559 mand, split by use and fuel type as well as the needed power at each time step.

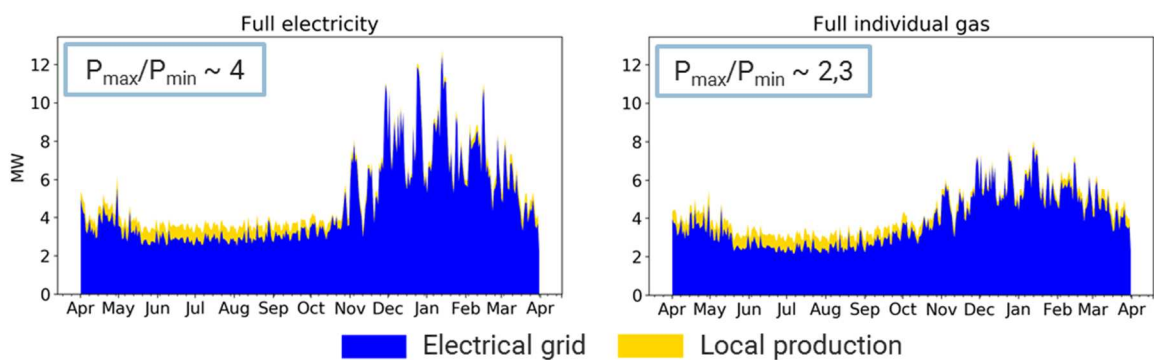
560 Figure 6 shows the different uses of fuel in the district. Even for the full gas scenarii, the part of electricity con-
561 sumption is still important due to the existing buildings, which are mainly equipped with electrical systems. In-
562 deed, when studying the thermal sensitivity of the district, the solutions based on gas (in the new buildings) are
563 insufficient to neutralize it. However, the “full individual/collective gas” solutions allow to reduce local electric

564 peaks between 40 to 57 % and the thermal sensibility from 4 to 2.3 (for the “full individual gas” scenario, Figure
 565 7) compared to the “full electricity” scenario.

566 When calculating PV production of the building roofs, the results show that these solutions are not able to reduce
 567 the electric peak in winter, but can lower the demand in summer. Furthermore, it was possible to determinate the
 568 archetypes of buildings where the systems are the most efficient in terms of self-consumption for the relevant
 569 scenarii. Figure 8 shows the self-consumption rate for each building in the district for the “full electricity” sce-
 570 nario. Here, it is better to give priority to PV systems to buildings composed of both residential and office areas,
 571 where the needs are better synchronized with the production.



572
 573 Figure 6 : Total final energy consumption per scenario



574
 575 Figure 7: Electrical power demand for the “full electricity” and “full individual gas” scenarii



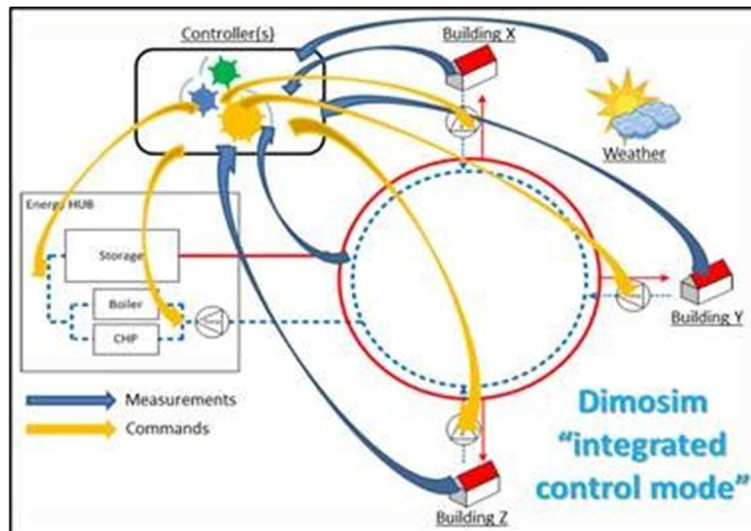
576

577

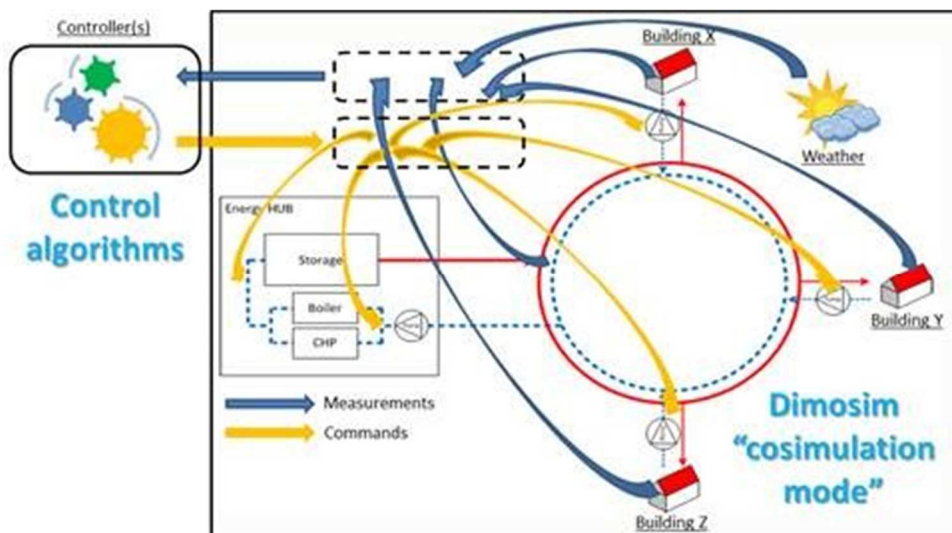
Figure 8: Self-consumption rate of the PV production for the “full electricity” scenario

578 **7.2 Co-simulation or emulation of an external controller**

579 It is possible to use DIMOSIM to evaluate algorithms or products (called “external controller”) that optimise and
 580 control the energy management in buildings or districts. To allow this, at each time step a client-server relation
 581 allows to exchange measurement data (from DIMOSIM to the external controller) and control data (from the ex-
 582 ternal controller to DIMOSIM) while coordinating the operation of both tools. The data exchange is based on a
 583 socket package in Python. A DIMOSIM specific API has been implemented to allow a standardised exchange
 584 protocol of data. One or several variables of the process are measured by sensors that are connected to the con-
 585 troller. The latter compares the variable to be controlled with a current set point. The algorithm will then calcu-
 586 late the necessary controller outputs for controlling the actuators of the process to be controlled. Figure 9 shows
 587 the two implemented layouts of simulation in DIMOSIM: (a) represents the standard control with all controllers
 588 implemented in DIMOSIM (standard) while (b) illustrates the external control mode in which one or several con-
 589 trollers are externalised (via emulation or co-simulation). The control actions (in yellow) can take two forms: ei-
 590 ther low-level signals such as a valve position, a command for the burner of a boiler, a pump or high-level sig-
 591 nals in the form of set points (assuming a low-level controller applying them).



(a)



(b)

592

593

594

595

596 Figure 9: Typical layout of control in simulation (a: mode with integrated control, b: plugin mode with external controller)

597 In E2District project (H2020), DIMOSIM has been connected to several external controllers. The objectives in
 598 this project were to develop a cloud-based tool to improve energy, environmental and economic performances of
 599 District Heating and Cooling (DHC) networks in districts. Three use cases were developed, connecting DI-
 600 MOSIM with tools for:

- 601 - Tool 1: Testing control strategies on DIMOSIM before applying them in real districts. In this case, a key
 602 feature was the ability to implement into DIMOSIM the digital twin of an existing DHN with its EMS so
 603 that the controller can be directly deployed after testings on the real installation.

- Tool 2: Optimizing the energy hub load to satisfy operational objectives, like minimizing operation costs. Scheduled set-points are sent to DIMOSIM, which provides thermal hub profiles, in order to create an optimisation loop to reach the objectives.
- Tool 3: Testing behaviour demand responses to evaluate the flexibility potential in district. Different thermal set point schedules are sent for various building zones in DIMOSIM to evaluate the behavioural model, controlling either the emitter valve command (real or high-level control) or the zone temperature set-point (ideal or high-level control).

All these co-simulations were tested and used on three demonstration sites from different countries, after a site-specific calibration process (on building properties, network insulation and production plants) to get as close as possible to reality.

Figure 10 represents the district heating network of a campus in Ireland, composed of one cogeneration plant (CHP), two boilers and a storage under one operating mode: heating production from the generators. Tool 1 is here able to apply a control strategy by acting on set points, valves or signals for heat production. Figure 11 shows the simulation of the site and its response to building demand. On the upper plot the district supply and return temperatures as well as the storage temperatures are shown. During morning, the heating demand from buildings rises and so the supply temperature. The storage is used at its maximum before turning the CHP on. The storage charge with the CHP only happens when the demand is lower around 11:00. The middle plot shows the activation of the different operating mode and generators. Finally the bottom plot presents the respecting loads.

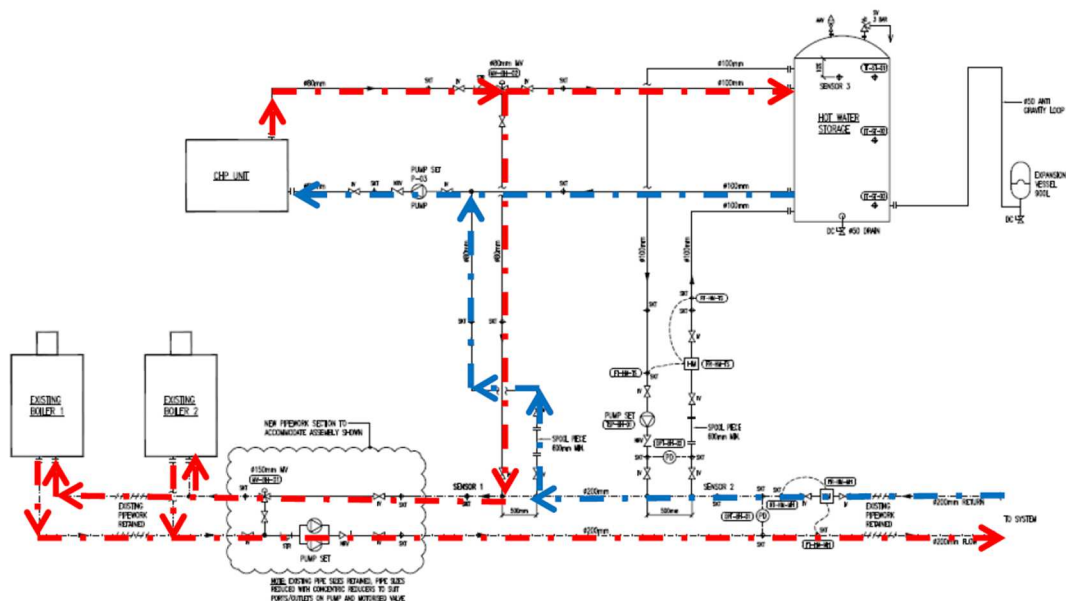
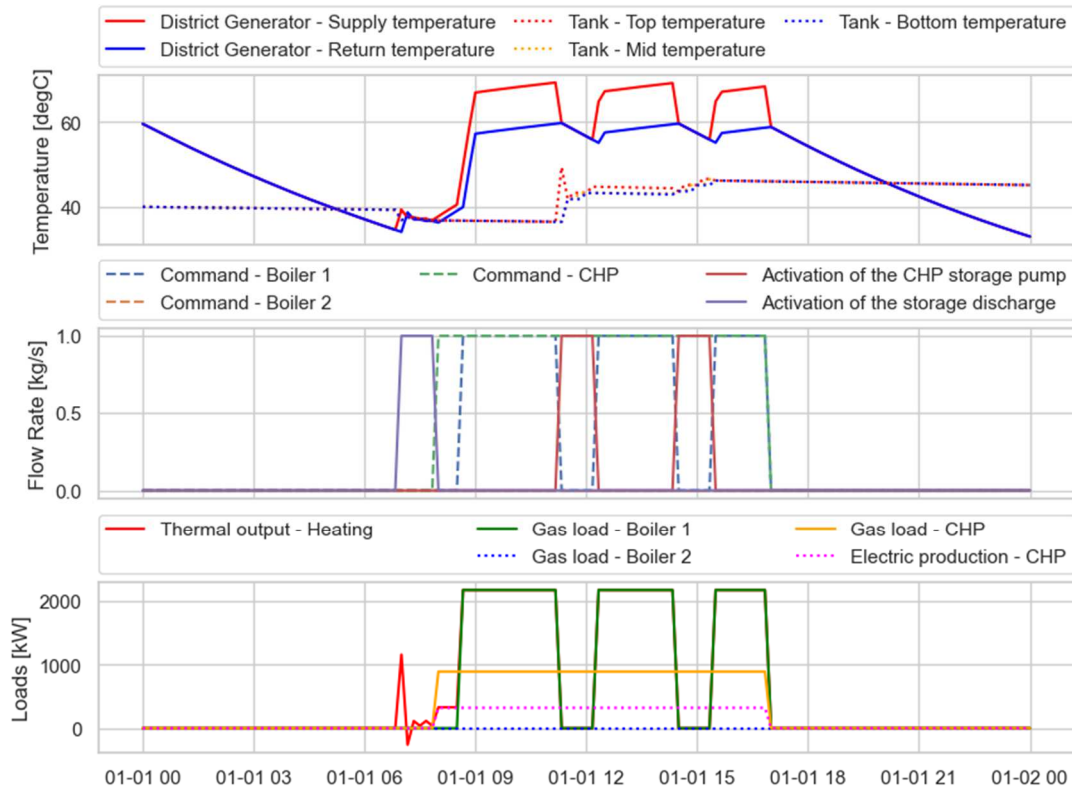


Figure 10: Ireland site operation mode: Heating with CHP and boilers



624

625

Figure 11: Evolution of states in the Ireland site under the strategy of the tool 1

626

A collateral benefit of this emulated testing procedure (besides energy or cost optimization purposes) is the possibility to improve Fault Detection & Diagnosis (FDD). Simulation offers then a very convenient environment for implementing various bugs within the physical models, and then being able to improve FDD algorithms.

628

629 7.3 DIMOSIM-microclimate

630

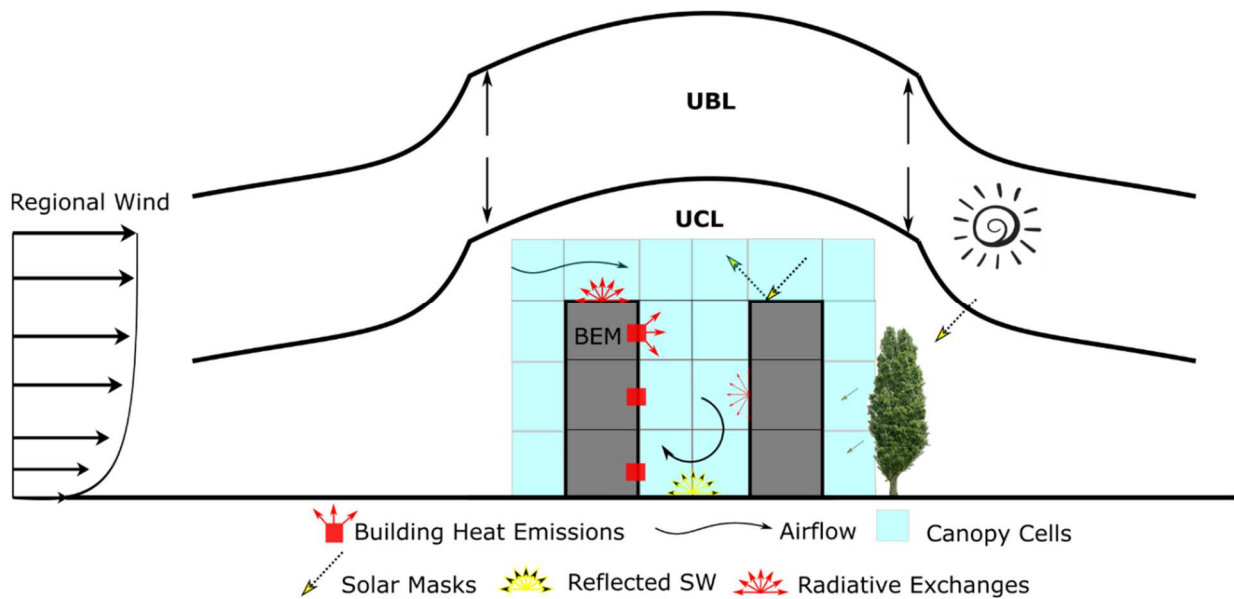
Urban overheating is a major challenge of the built environment related to increased energy consumption and peak electricity demand for cooling. Several sources highlight the need for microclimate integration in building energy studies ([16], [48]). In parallel, the implications of the so-called Urban Heat Island effect, including the deterioration of outdoor thermal comfort conditions, lead to the development of various urban mitigation strategies. The latter is employed either at the building level through energy conservation measures (ECMs) as in [3], to reduce energy use in buildings or to limit the anthropogenic heat emissions, or at the neighbourhood scale [49] to limit heat stress and to establish improved boundary conditions for the indoor environment. However, an UBEM that encompasses the urban building energy demand, the local microclimate conditions and the integration of district energy systems concurrently lacks from the literature.

638

639 7.3.1 DIMOSIM-microclimate workflow

640 DIMOSIM-microclimate represents a special module of the tool which is based on the co-simulation approach.
641 The developed model aims to assess the physical interactions between buildings- energy systems and local mi-
642 croclimate, considering the site-specific effects. It operates at the neighbourhood scale for annual simulations.
643 We introduce an intermediate precision model by actively coupling a set of validated models: a solar radiation
644 model (SOLENE [50]), a reduced-order urban dispersion code, both integrated under a zonal approach (ENVI-
645 BATE [51]) and the core thermal zone model of DIMOSIM (detailed in 5.3.2). Moreover, a further asynchronous
646 coupling with a simplified meso-model (UWG [52]) is tested to assess the boundary layer UHI. The developed
647 module, as shown in Figure 12 extends the simulation capabilities by:

- 648 - Detailed calculations in a fine mesh of direct and diffuse solar irradiance components, enhanced with
- 649 multi-reflections (radiosity method) and radiative exchanges between urban surfaces and the sky,
- 650 - Flow distribution and wind speed magnitude around buildings,
- 651 - Canopy air temperature magnitude, stratification and distribution.



652
653

Figure 12: Schematic representation of DIMOSIM-microclimate module.

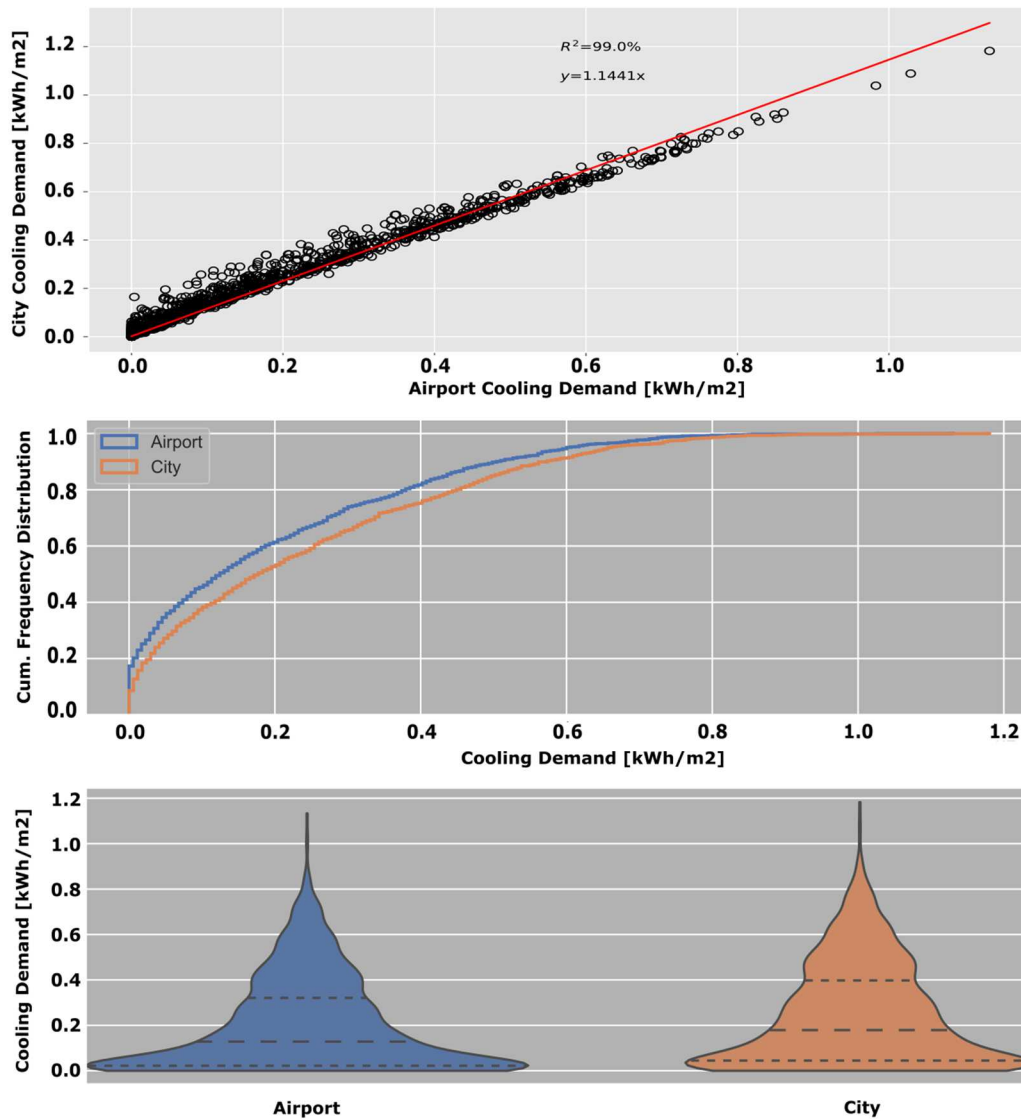
654 Given the imported data, a first step exchange between the tools is performed to index the building footprints, as
655 well as to expand the simulation domain of DIMOSIM from single buildings to the complete urban form (roads,
656 sidewalks, etc.). In a further step, the required sub-meshes (solar triangular, airflow hexahedral), which are nec-
657 essary for the detailed solar calculations and the airflow distribution, are automatically generated. The core cal-
658 culation is executed by employing the co-simulation approach for a synchronous coupling scheme as given in de-

659 tail in [15]. The control objects (Figure 9) are the thermal zones in which the microclimate module provides the
660 average outdoor air temperature of the adjacent canopy cells along with the incident shortwave irradiance after
661 reflection and the radiative fluxes between the urban surfaces. Simultaneously, the local generator (in split sys-
662 tems case) and the thermal zone objects calculate the heat emissions from buildings, supplying with their respec-
663 tive fluxes the energy balance for each canopy cell.

664 7.3.2 *Neighbourhood Case study*

665 An indicative case study was performed using a simplified urban archetype characterized as discontinuous row
666 of mid-rise high-density urban canyon for the city of La Rochelle, France. The thermal and optical properties of
667 the neighbourhood case study along with the simulation parameters can be found in [53]. Two simulation scenar-
668 ii were compared: a standalone DIMOSIM simulation and a microclimate one, designated respectively as “air-
669 port” and “city”. The first employs typical weather data as boundary conditions while the second is based on the
670 coupling scheme between DIMOSIM and EnviBatE enhanced with modified meteorological data from UWG.

671 Figure 13 plots the cooling demand of the neighbourhood for the standalone model (airport) and the microcli-
672 mate one (city) Overall, the comparison between them presents a rise of 19%, in terms of relative difference,
673 when the microclimate is considered. Both the violin plot and the cumulative frequency diagrams exhibit signifi-
674 cant variations. The first shows the shift of the quartiles towards increased values of cooling demand, corre-
675 sponding to a relative increase of 51%, 28% and 20% under the microclimate model. In parallel, it indicates the
676 distribution discrepancies especially for low values. The number of time steps where the cooling demand from
677 zero (airport scenario) turns into a positive one (microclimate scenario) increases by 9%. The cumulative fre-
678 quency plot shows the steadily increased cooling demand in the microclimate scenario for non-null values. How-
679 ever, both figures present low discrepancies in terms of absolute values. Similar outcomes have been reported in
680 [54] for low cooling needs of referenced buildings.

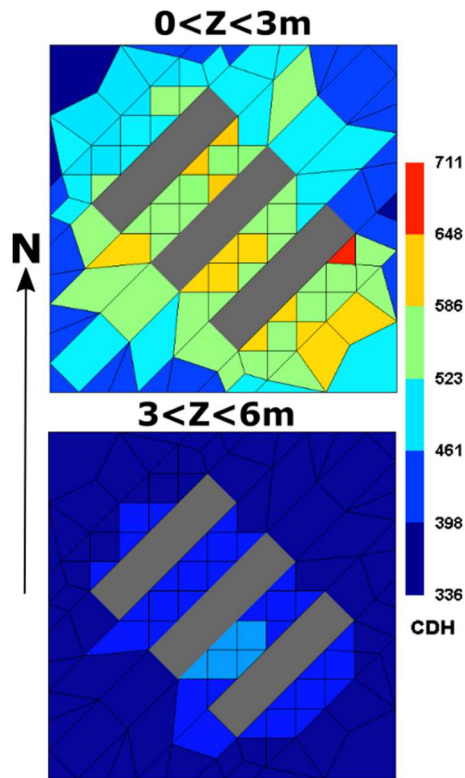


681
682
683

Figure 13: Violin plots (bottom), cumulative frequency distribution (mid), and correlation (top) between standalone DI-MOSIM (airport) and DIMOSIM -microclimate (city).

684
685
686
687
688
689
690
691
692
693

The distribution of the Cooling Degree Hours (CDH) for every canopy cell during the cooling period is depicted in Figure 14, given a base temperature of 26°C. This indicator is widely used in the building energy domain and is related to local urban climate modifications. In both canopy layers is evident the increased CDH index inside the canyons and around the buildings. The canyon orientation, situated perpendicularly to the mean wind direction of the meteorological data during the cooling period, acts as a barrier to the prevailing wind associating the low wind circulation with overcharged canopy cells. More in detail, the canopy cells adjacent to South oriented facades present a considerable increase in CDH index. This is correlated with higher surface temperatures and reduced air circulation in the lee-side of the thermal zones, concluding to heat trapping. The corresponding meteorological value is 350 CDH, indicating that locally the impact of the buildings can double the thermal discomfort of the studied area.



694
695
696

Figure 14: Distribution of CDH for the first and second canopy layers during the entire cooling period simulated with DIMOSIM -microclimate.

697

8 Conclusion

698
699
700
701
702
703
704
705
706
707
708
709
710

In this paper, DIMOSIM, a transient energetic simulation platform at neighbourhood, district and territory scale is presented. The structure of this platform was chosen in order to allow case studies on several geographic scales for the optimisation of energy design concepts and energy management strategies. It is modular and considers a wide range of these energy concepts (refurbishment of buildings, district heating/cooling networks, district electrical networks, choice of local energy system, optimisation of central plants production...) but also to ease implementation of models. These models can be with high or low level of detail to adapt the global model to the simulation objective and scene characteristics. It can then be used to assist several district stakeholders as city energy managers or distribution system operators in their choices and actions. Depending on the case, simplified models can be used when few input data are available or when a compromise between simulation time and accuracy is expected. For the solar radiation computation, the level of detail must be chosen according to the district morphology to achieve an acceptable range of uncertainty.

To date, the platform was only validated against the BESTEST cases for the building model and partially against real data from the different international projects in which DIMOSIM takes part. More work is needed to com-

711 plete this validation, including the data inference procedure which can be seen as a pre-processor of the plat-
712 form. This validation is underway, with work on the uncertainty propagation of input parameters ([55], [56]) and
713 comparison with other UBEM tools.

714 .

715 As a future perspective, DIMOSIM could be completed with a life cycle assessment calculation. With the devel-
716 opment of new thermal regulations and environmental certifications at district level this kind of calculation will
717 be soon necessary. In the same way the link with BIM/DIM (Building/District Information Model) models could
718 be of a major interest to get automatically all the materials information as more and more building projects are
719 using it.

720 **9 Acknowledgments**

721 *Acknowledgments* - The application example has been taken from the European E2District and French SMART
722 Montpellier projects, therefore the authors would like to thank them for their results.

723 *Authors contributions* - EG wrote the paper with significant conceptual input as well as critical feedback from all
724 co-authors. VP, PR developed the base simulation program in Matlab and YA, VP, PR implemented DIMOSIM
725 in an object-oriented way to Python. WK, EH, EG and GEK contributed to further develop DIMOSIM and inte-
726 grate various modeling components. GEK & PR conceptualized and developed the DIMOSIM-Microclimate
727 package and contributed to the original draft.

728

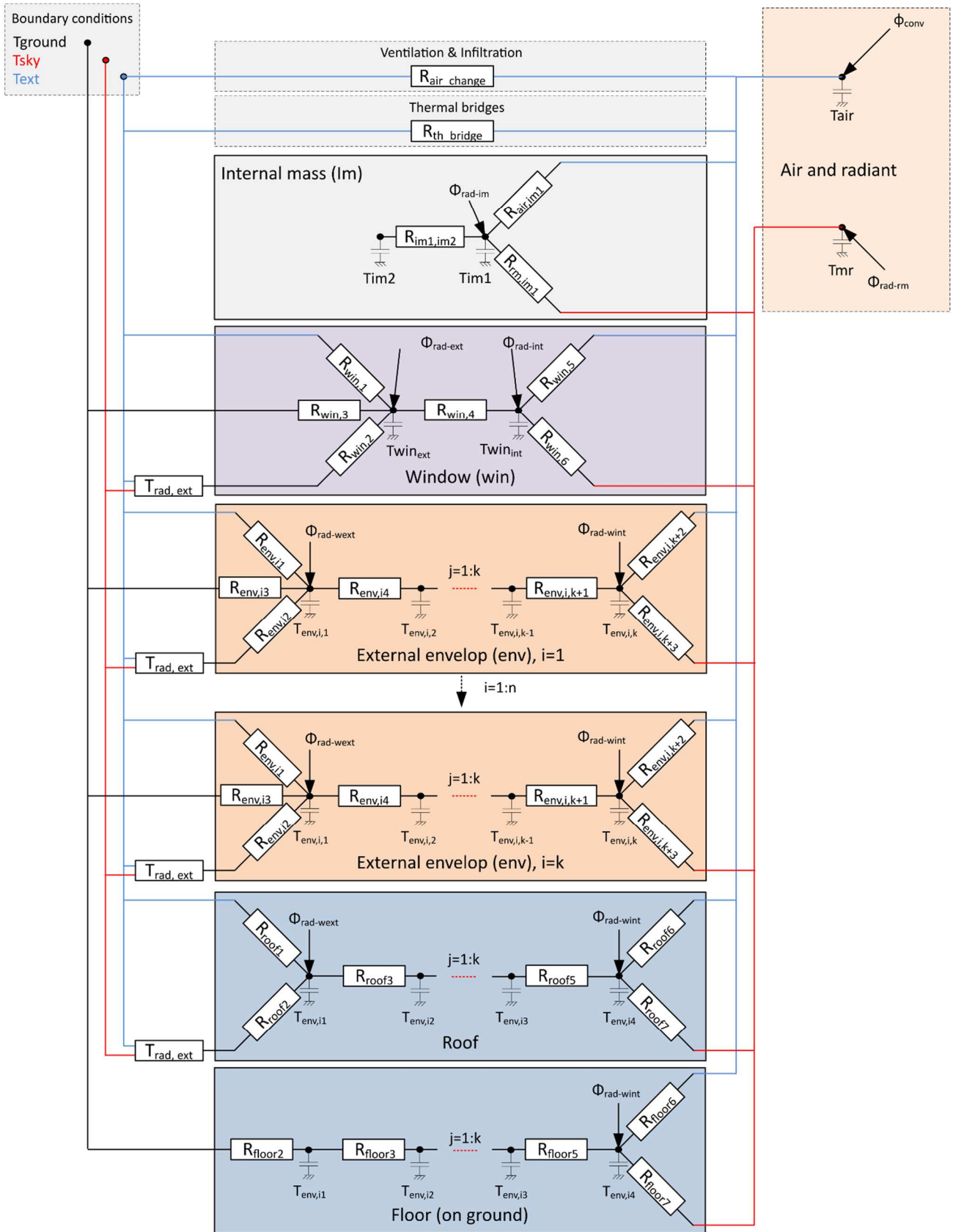


Figure 15: R:C_j thermal model

730

731

References

- [1] International Energy Agency, Ed., *Transition to sustainable buildings: strategies and opportunities to 2050*. Paris: IEA Publ, 2013.
- [2] United Nations, “World Urbanization Prospects - The 2018 Revision,” United Nations, Department of Economic and Social Affairs, Population Division, New York, ST/ESA/SER.A/366, 2018. [Online]. Available: <https://population.un.org/wup/Publications/>
- [3] A. Synnefa *et al.*, “Minimizing the energy consumption of low income multiple housing using a holistic approach,” *Energy Build.*, vol. 154, pp. 55–71, Nov. 2017, doi: 10.1016/j.enbuild.2017.07.034.
- [4] H. Í. Tol and S. Svendsen, “Improving the dimensioning of piping networks and network layouts in low-energy district heating systems connected to low-energy buildings: A case study in Roskilde, Denmark,” *Energy*, vol. 38, no. 1, pp. 276–290, Feb. 2012, doi: 10.1016/j.energy.2011.12.002.
- [5] E. Guelpa, C. Toro, A. Sciacovelli, R. Melli, E. Sciubba, and V. Verda, “Optimal operation of large district heating networks through fast fluid-dynamic simulation,” *Energy*, vol. 102, pp. 586–595, May 2016, doi: 10.1016/j.energy.2016.02.058.
- [6] S. Freitas, C. Catita, P. Redweik, and M. C. Brito, “Modelling solar potential in the urban environment: State-of-the-art review,” *Renew. Sustain. Energy Rev.*, vol. 41, pp. 915–931, Jan. 2015, doi: 10.1016/j.rser.2014.08.060.
- [7] R. Compagnon, “RADIANCE: a simulation tool for daylighting systems.” LESO-PB, EPFL, 2001.
- [8] A. Hénon, P. G. Mestayer, J.-P. Lagouarde, and J. A. Voogt, “An urban neighborhood temperature and energy study from the CAPITOU experiment with the SOLENE model,” *Theor. Appl. Climatol.*, vol. 110, no. 1, pp. 177–196, Oct. 2012, doi: 10.1007/s00704-012-0615-0.
- [9] E. Walther and Q. Goestchel, “The P.E.T. comfort index: Questioning the model,” *Build. Environ.*, vol. 137, pp. 1–10, Jun. 2018, doi: 10.1016/j.buildenv.2018.03.054.
- [10] K. M. Luc, R. Li, L. Xu, T. R. Nielsen, and J. L. M. Hensen, “Energy flexibility potential of a small district connected to a district heating system,” *Energy Build.*, vol. 225, p. 110074, Oct. 2020, doi: 10.1016/j.enbuild.2020.110074.
- [11] S. Troitzsch *et al.*, “Optimal electric-distribution-grid planning considering the demand-side flexibility of thermal building systems for a test case in Singapore,” *Appl. Energy*, vol. 273, p. 114917, Sep. 2020, doi: 10.1016/j.apenergy.2020.114917.
- [12] A. Vandermeulen, B. van der Heijde, and L. Helsen, “Controlling district heating and cooling networks to unlock flexibility: A review,” *Energy*, vol. 151, pp. 103–115, May 2018, doi: 10.1016/j.energy.2018.03.034.
- [13] G. Sandou, S. Font, S. Tebbani, A. Huret, and C. Mondon, “Predictive Control of a Complex District Heating Network,” in *44th IEEE Conference on Decision and Control, and the European Control Conference 2005*, Seville, Spain, 2005, pp. 7372–7377. doi: 10.1109/CDC.2005.1583351.
- [14] J. Allegrini, V. Dorer, and J. Carmeliet, “Influence of the urban microclimate in street canyons on the energy demand for space cooling and heating of buildings,” *Energy Build.*, vol. 55, pp. 823–832, Dec. 2012, doi: 10.1016/j.enbuild.2012.10.013.
- [15] G.-E. Kyriakodis, “Development of a coupled simulation tool for urban building energy demand, district energy systems and microclimate modeling,” Université de La Rochelle, 2020.
- [16] J. Allegrini, K. Orehounig, G. Mavromatidis, F. Ruesch, V. Dorer, and R. Evins, “A review of modelling approaches and tools for the simulation of district-scale energy systems,” *Renew. Sustain. Energy Rev.*, vol. 52, no. C, pp. 1391–1404, 2015.
- [17] J. Fonseca, T.-A. Nguyen, A. Schlueter, and F. Maréchal, “City Energy Analyst (CEA): Integrated framework for analysis and optimization of building energy systems in neighborhoods and city districts,” *Energy Build.*, vol. 113, Dec. 2015, doi: 10.1016/j.enbuild.2015.11.055.
- [18] T. Berthou, B. Duplessis, P. Rivière, P. Stabat, D. Casetta, and D. Marchio, “SMART-E: A Tool For Energy Demand Simulation And Otimization At The City Scale,” in *Proceedings of BS2015: 14th Conference of IBPSA*, Hyderabad, India, Dec. 2015, pp. 1782–1789.
- [19] D. Robinson *et al.*, “CITYSIM: Comprehensive Micro-Simulation of Resource Flows For Sustainable Urban Planning,” in *Proceedings of BS2009: 11th Conference of International Building Performance Simulation Association*, Glasgow, Scotland, 2009, pp. 1083–1090.
- [20] Y. Chen, T. Hong, and M. A. Piette, “Automatic generation and simulation of urban building energy models based on city datasets for city-scale building retrofit analysis,” *Appl. Energy*, vol. 205, pp. 323–335, Nov. 2017, doi: 10.1016/j.apenergy.2017.07.128.
- [21] D. Saelens *et al.*, “Towards a DESTEST: a District Energy Simulation Test Developed in IBPSA Project 1,” in *Proceedings of Building Simulation 2019: 16th Conference of IBPSA*, Rome, Italy, 2019, pp. 3569–3577. doi: 10.26868/25222708.2019.210806.

- [22] P. Riederer, V. Partenay, N. Perez, C. Nocito, R. Trigance, and T. Guiot, "Development Of A Simulation Platform For The Evaluation Of District Energy System Performances," in *Proceedings of BS2015: 14th Conference of International Building Performance Simulation Association*, Hyderabad, India, 2015, pp. 2499–2506.
- [23] European Commission - CORDIS and RINA CONSULTING SPA (Coordinator), "RESILIENT: coupling RENEwable, Storage and ICTs, for Low carbon Intelligent Energy maNagementT at district level," European Commission, CORDIS, FP7-2012-NMP-ENV-ENERGY-ICT-EeB, 2012. Accessed: May 16, 2019. [Online]. Available: <https://cordis.europa.eu/project/rcn/104392/factsheet/en>
- [24] G. Manganini, S. Rivero, and K. Kouramas, "A graph-based optimization framework for the Energy Management of District Systems," in *2019 IEEE 58th Conference on Decision and Control (CDC)*, Dec. 2019, pp. 7252–7257. doi: 10.1109/CDC40024.2019.9029679.
- [25] Y. Nzengue *et al.*, "Planning city refurbishment: An exploratory study at district scale how to move towards positive energy districts – approach of the SINFONIA project," in *2017 International Conference on Engineering, Technology and Innovation (ICE/ITMC)*, Jun. 2017, pp. 1394–1400. doi: 10.1109/ICE.2017.8280045.
- [26] F. Fuligni and F. Centeno, "THERMOSS," European Union's Horizon 2020 research and innovation, G.A. n° 723562, 2016. [Online]. Available: <https://thermoss.eu/>
- [27] A. Rogeau, R. Girard, Y. Abdelouadoud, M. Thorel, and G. Kariniotakis, "Joint optimization of building-envelope and heating-system retrofits at territory scale to enhance decision-aiding," *Appl. Energy*, vol. 264, p. 114639, Apr. 2020, doi: 10.1016/j.apenergy.2020.114639.
- [28] G.-E. Kyriakodis, P. Riederer, and E. Bozonnet, "Towards the development of a coupled model for district simulation: buildings, energy systems and microclimate co-simulation," in *IBPSA France 2018 (Conférence Francophone de l'International Building Performance Simulation Association)*, Bordeaux, France, May 2018, vol. hal-02005502.
- [29] E. Garreau, T. Berthou, B. Duplessis, V. Partenay, and D. Marchio, "Urban-scale Energy Simulation: A Development Of A Novel Method For Parsimonious Modelling - The Example Of Solar Shading Model Calculation," in *Proceedings of Building Simulation 2019: 16th Conference of IBPSA*, Rome, Italy, 2019, pp. 3258–3265. doi: 10.26868/25222708.2019.210344.
- [30] A. Mailhac *et al.*, "Articulation d'un logiciel de simulation énergétique et d'un logiciel d'ACV à l'échelle quartier, illustration à travers une étude de cas," in *Conférence IBPSA France*, Marne-la-Vallée, France, 2016, p. 9.
- [31] M. Brugeron, R. Peter, F. Wurtz, and M. Yves, "An Approach of Model-based Predictive Control For Energy Consumption at a Community Level fo," in *Proceedings of Building Simulation 2019: 16th Conference of IBPSA*, Rome, Italy, 2019, pp. 2771–2778. doi: 10.26868/25222708.2019.210143.
- [32] P. Schetelat, "Urban data imputation using multi-output multi-class classification," presented at the uSIM2020, Scotland, 2020.
- [33] Efficacity - Institut de Recherche & Développement, "Outils d'Efficacity," *Efficacity - Institut de Recherche & Développement*, 2020. <https://www.efficacity.com/la-chaine-doutils-defficacity/> (accessed Dec. 14, 2020).
- [34] S. Behnel, R. Bradshaw, C. Citro, L. Dalcin, D. S. Seljebotn, and K. Smith, "Cython: The Best of Both Worlds," *Comput. Sci. Eng.*, vol. 13, no. 2, pp. 31–39, Mar. 2011, doi: 10.1109/MCSE.2010.118.
- [35] S. Georgiou, M. Kechagia, and D. Spinellis, "Analyzing Programming Languages' Energy Consumption: An Empirical Study," in *PCI 2017: Proceedings of the 21st Pan-Hellenic Conference on Informatics*, Sep. 2017, pp. 1–6. doi: 10.1145/3139367.3139418.
- [36] UIUC, "EnergyPlus Documentation : Engineering Reference." US Department of Energy, 2015. [Online]. Available: https://energyplus.net/sites/default/files/pdfs_v8.3.0/EngineeringReference.pdf
- [37] T. Kasuda, P. R. Archenbach, and United States - Office of Civil Defense, "Earth Temperature and Thermal Diffusivity at Selected Stations in the United States," National Bureau of Standards (Washington, DC), 8972, 1965.
- [38] IGN, "BDTOPO@ | IGN - Espace professionnel." <http://professionnels.ign.fr/bdtopo> (accessed Dec. 17, 2018).
- [39] C. Gay and P. Schetelat, "Low carbon district - Energy and behaviour modeling," in *Proceedings of the4th Workshop organised by the EEB Data Models Community ICT for Sustainable Places*, Nice, France, 2013, pp. 33–45. [Online]. Available: http://www.sustainableplaces.eu/wp-content/uploads/2017/01/Proceedings-of-4th-EEB-Data-Models-Community-workshop_ICT-for-Sustainable-Places_2013.pdf
- [40] INSEE, "Enquête emploi du temps en 2010," INSEE, Insee Résultats N°130, 2012. [Online]. Available: <https://www.insee.fr>
- [41] J. L. Dréau, M. Vellei, and S. Martinez, "Pilotage du levier de flexibilité a l'échelle du quartier - analyse de sensibilité," presented at the Conférence IBPSA France, Nov. 2020. Accessed: Jul. 05, 2021. [Online]. Available: <https://hal-univ-rochelle.archives-ouvertes.fr/hal-03077521>

- [42] A. Breitwiller, R. Lahrech, T. Rieser, and B. Rozel, “Projet PECOIC -Prise en compte du comportement des occupants et incertitudes associées en phase conception de bâtiments en phase conception,” ADEME, CSTB, Enertech, 2019.
- [43] E. Vorger, “Étude de l’influence du comportement des habitants sur la performance énergétique du bâtiment,” Ecole Nationale Supérieure des Mines de Paris, 2014. Accessed: Jul. 15, 2021. [Online]. Available: <https://pastel.archives-ouvertes.fr/tel-01144461>
- [44] C. Reinhart and P.-F. Breton, “Experimental validation of 3DS MAX design 2009 and DAYSIM 3.0,” in *Proceedings of BS2011: 12th Conference of International Building Performance Simulation Association*, Glasgow, Scotland, Jul. 2009, pp. 1514–1521. doi: 10.1582/LEUKOS.2009.06.01001.
- [45] N. Perez, P. Riederer, C. Inard, and V. Partenay, “Thermal Building Modelling Adapted To District Energy Simulation,” in *Proceedings of BS2015: 14th Conference of International Building Performance Simulation Association*, Hyderabad, India, Dec. 2015, pp. 270–277. doi: 10.13140/RG.2.1.3714.2163/1.
- [46] European Commission, “Energy efficiency assessment and energy monitoring results,” Thermoss Project (Building and district thermal retrofit and management solutions); Grant agreement nb: 723562 (Horizon 2020 research and innovation programme), Deliverable D6.2, Public THERMOSS-WP6-DEL-D6.2-EXERGY-20200229, 2016.
- [47] S. Y. Abdelouadoud, R. Girard, T. Guiot, and F.-P. Neirac, “Planning-oriented yearly simulation of energy storage operation in distribution system for profit maximization, voltage regulation and reserve provisioning,” in *22nd International Conference and Exhibition on Electricity Distribution - CIRED 2013*, Stockholm, Sweden, Jun. 2013, p. Paper 1243-4 pages-ISBN 978-1-84919-732-8. doi: 10.1049/cp.2013.1139.
- [48] M. Santamouris, *Energy and climate in the urban built environment*. Routledge, 2013.
- [49] G. Kyriakodis and M. Santamouris, “Using reflective pavements to mitigate urban heat island in warm climates-Results from a large scale urban mitigation project,” *Urban Clim.*, vol. 24, pp. 326–339, 2018.
- [50] F. Miguet and D. Groleau, “A daylight simulation tool for urban and architectural spaces—application to transmitted direct and diffuse light through glazing,” *Build. Environ.*, vol. 37, no. 8–9, pp. 833–843, 2002.
- [51] A. Gros, E. Bozonnet, and C. Inard, “Cool materials impact at district scale—Coupling building energy and microclimate models,” *Sustain. Cities Soc.*, vol. 13, pp. 254–266, 2014.
- [52] B. Bueno, L. Norford, J. Hidalgo, and G. Pigeon, “The urban weather generator,” *J. Build. Perform. Simul.*, vol. 6, no. 4, pp. 269–281, 2013.
- [53] G.-E. Kyriakodis, E. Bozonnet, and P. Riederer, “Quantifying the impact of urban microclimate in detailed urban building energy simulations,” presented at the Proceedings of Building Simulation 2019: 16th Conference of IBPSA, Rome, Italy, 2019.
- [54] M. Santamouris, “Recent progress on urban overheating and heat island research. Integrated assessment of the energy, environmental, vulnerability and health impact. Synergies with the global climate change,” *Energy Build.*, vol. 207, p. 109482, 2020.
- [55] L. Lefort, “Développement d’une méthode de référence pour la validation des outils de simulation énergétique des bâtiments à l’échelle urbaine,” These en préparation, Université Paris sciences et lettres, 2019. Accessed: Nov. 02, 2020. [Online]. Available: <http://www.theses.fr/s231237>
- [56] L. Lefort *et al.*, “Development of a methodology of validation for urban building energy models and application to French residential consumption,” Edenbourg (on line), United Kingdom, Nov. 2020. Accessed: Jul. 15, 2021. [Online]. Available: <https://hal.archives-ouvertes.fr/hal-03202728>